

Nonlinear free vibration of FG-CNT reinforced composite plates

Mostafa Mirzaei*¹ and Yaser Kiani²

¹Department of Mechanical Engineering, Faculty of Engineering, University of Qom, Qom, Iran

²Faculty of Engineering, Shahrekord University, Shahrekord, Iran

(Received July 13, 2017, Revised August 20, 2017, Accepted August 21, 2017)

Abstract. Present paper deals with the large amplitude flexural vibration of carbon nanotube reinforced composite (CNTRC) plates. Distribution of CNTs as reinforcements may be uniform or functionally graded (FG). The equivalent material properties of the composite media are obtained according to a refined rule of mixtures which contains efficiency parameters. To account for the large deformations, von Kármán type of geometrical nonlinearity is included into the formulation. The matrix representation of the governing equations is obtained according to the Ritz method where the basic shape functions are written in terms of the Chebyshev polynomials. Time dependency of the problem is eliminated by means of the Galerkin method and the resulting nonlinear eigenvalue problem is solved employing a direct displacement control approach. Results are obtained for completely clamped and completely simply supported plates. Results are first validated for the especial cases of FG-CNTRC and cross-ply laminated plates. Afterwards, parametric studies are given for FG-CNTRC plates with different boundary conditions. It is shown that, nonlinear frequencies are highly dependent to the volume fraction and dispersion profiles of CNTs. Furthermore, mode redistribution is observed in both simply supported and clamped FG-CNTRC plates.

Keywords: functionally graded; nonlinear free vibration; CNTRC; rectangular plate; Ritz method

1. Introduction

Carbon nanotubes are known as an excellent reinforcement for the composites due to their outstanding thermal, mechanical and electrical properties (Liew *et al.* 2015). As reinforcements, CNTs may be distributed uniformly or according to a functionally graded pattern in a matrix (Kwon *et al.* 2013). As a result a novel class of materials known as functionally graded carbon nanotube reinforced composites (FG-CNTRC) may be achieved which have the properties of FGMs and CNTs together.

Shen (2009) was the first who compared the structural behaviour of FG-CNTRC and uniformly distributed (UD)-CNTRC rectangular plates under the action of uniform lateral pressure. It is shown that, bending moments may be alleviated significantly through usage of CNTs in a functionally graded pattern. Following this work, various researches are reported up to now on the behaviour of composites reinforced with functionally graded CNTs. In the next, an overview of the works on free vibration of FG-CNTRC plates and panels is provided.

Kiani (2016a) investigated the free vibration characteristics of moderately thick FG-CNTRC rectangular plates integrated with two identical piezoelectric layers perfectly bonded to the top and bottom surfaces of the plate. Both open circuit and closed circuit electrical boundary conditions are taken into consideration for the plate and mechanical boundary conditions are chosen arbitrarily. Kiani (2017a) obtained the natural frequencies and mode

shapes of FG-CNTRC rectangular plates located on point supported. The constraints of point supports are inserted into the total functional of the plate using the concept of the Lagrangian multipliers. Based on the concept of negative stiffness, Mirzaei and Kiani (2016a) obtained the frequencies of rectangular FG-CNTRC plates containing a centric cut-out using the conventional Ritz method. Free vibrations of cylindrical panels and spherical panels are studied by Mirzaei and Kiani (2016b), Kiani (2017d) using the Ritz method. In the analysis of Mirzaei and Kiani (2016b) the Chebyshev polynomials are used as the basic functions to construct the shape functions whereas the analysis of Kiani (2017d) uses the Gram-Schmidt process to generate an orthogonal set of shape functions suitable for arbitrary combinations of boundary conditions. Zhang *et al.* (2015a) obtained the mode shapes and natural frequencies of triangular plates using the first order shear deformation theory and element-free IMLS-Ritz method. Natarajan *et al.* (2014) developed a finite element formulation based on the QUAD-8 shear flexible element to analyse the free vibration of FG-CNTRC plates and sandwich plates with FG-CNTRC face sheets based on a higher order shear and normal deformable plate theory. Numerical results of this study are confined to plates with simply supported edges. Based on an element free IMLS Ritz formulation, Zhang *et al.* (2015b) obtained the natural frequencies of FG-CNTRC rectangular plates resting on a two parameters elastic foundation.

Malekzadeh and Zarei (2014) developed a two dimensional generalised differential quadrature solution to obtain the natural frequencies of arbitrary quadrilateral plates containing FG-CNTRC layers. Zhang *et al.* (2015c) obtained the natural frequencies of skew plates using a

*Corresponding author, Assistant Professor
E-mail: m.mirzaei@qom.ac.ir

mesh-free method based on the first order shear deformation plate theory. Kiani (2016b) applied the Ritz method to the total functional of a skew FG-CNTRC plate to obtain the natural frequencies of the plate with arbitrary boundary conditions. In this research a transformation is provided to use an oblique coordinate system instead of the conventional Cartesian system. Garcia-Macias *et al.* (2016) also obtained the natural frequencies of skew plates. The shell element is formulated in an oblique coordinates. The theoretical development rests upon the Hu-Washizu principle.

In comparison to linear free vibration of FG-CNTRC plates, less attention is devoted to nonlinear free vibration. This is expected due to the geometrically nonlinear nature of the governing equations for large amplitude vibrations which makes the solution method more complicated. Wang and Shen (2011, 2012a, b) and Shen and Xiang (2014) applied the two step perturbation technique to obtain the nonlinear frequencies of an FG-CNTRC rectangular plate, sandwich plates with FG-CNTRC face sheets and FG-CNTRC cylindrical panel. Solution method of these researches is suitable for plates which are simply supported all around in flexure while are movable or immovable in axial direction. Various effects such as elastic foundation and thermal environment and temperature dependency of constituents are also taken into account. Fan and Wang (2016) investigated the effects of matrix cracking on linear and nonlinear frequencies of completely simply supported FG-CNTRC rectangular plates using the von Kármán plate formulation and a two step perturbation technique.

As the above literature survey reveals, nonlinear free vibration of rectangular FG-CNTRC plates has been the subject of a few researches. However all of those researches are limited to plates which are simply supported all around and the nonlinear vibration mode shape and linear vibration mode shape are chosen the same. The present research proposes a solution method based on the Chebyshev-Ritz method suitable for arbitrary combinations of boundary conditions in FG-CNTRC plates. However, results of this study are confined to plates with simply supported or clamped edges. Numerical results are compared with the available data in the open literature to assure the accuracy and correctness of the developed formulation. Afterwards parametric studies are given to explore the influences of involved parameters on the nonlinear frequencies of the plate.

2. Basic formulation

Consider a composite plate reinforced with aligned single walled carbon nanotubes (SWCNT). As usual, thickness, width and length of the plate are denoted by, h , b and a , respectively. An orthogonal coordinate system is assigned to the center of the mid-plane of the plate. Therefore plate occupies the domain $-0.5a \leq x \leq +0.5a$, $-0.5b \leq y \leq +0.5b$, and $-0.5h \leq z \leq +0.5h$.

SWCNT as reinforcements may be uniformly distributed (UD) or functionally graded (FG) according to a prescribed dispersion for volume fraction of CNTs. This

Table 1 Volume fraction of CNTs as a function of thickness coordinate for various cases of CNTs distribution

CNTs Distribution	V_{CN}
UD CNTRC	V_{CN}^*
FG-O CNTRC	$2V_{CN}^* \left(1 - 2 \frac{ z }{h}\right)$
FG-X CNTRC	$4V_{CN}^* \frac{ z }{h}$
FG-V CNTRC	$V_{CN}^* \left(1 + 2 \frac{z}{h}\right)$

type of composite is referred to as functionally graded carbon nanotube reinforced composite (FG-CNTRC). Various types of functionally graded profiles may be considered for the FG-CNTRC. However due to their consistency with the fabrication processes, only linear distributions of volume fraction of CNT across the plate thickness have attracted attention. Three types of FG-CNTRC are considered in the present research which are FG-O, FG-V and FG-X.

In Table 1 distribution function of CNTs across the plate thickness is provided.

It is easy to check from Table 1 that, all of these types have the same value of volume fraction. The total volume fraction across the plate thickness in all of these cases is equal to V_{CN}^* . In FG-X type, distribution of CNT is maximum near the top and bottom surfaces whereas the mid-plane is free of CNT. For FG-O, however, top and bottom surfaces are free of CNTs and the mid-surface of the plate is enriched with CNTs. In FG-V type, the top surface is enriched with CNT and the bottom surface is free of CNT. In UD type, each surface of the plate through the thickness has the same volume fraction of CNTs.

Generally, the effective mechanical properties of the FG-CNTRC rectangular plate are obtained using the well-known homogenization schemes, such as Mori-Tanaka scheme (Shi *et al.* 2004) or the rule of mixtures (Fidelus *et al.* 2005). For the sake of simplicity, in the present research, the rule of mixtures is used to obtain the properties of the composite plate. However to account for the scale dependent properties of nanocomposite media, efficiency parameters are introduced. This approach has been used extensively for beams, plates and shells (Tohidi *et al.* (2017), Mohammadimehr *et al.* (2016) and Mosallaie Barzoki *et al.* 2015). Accordingly, the effective material properties may be written as

$$\begin{aligned}
 E_{11} &= \eta_1 V_{CN} E_{11}^{CN} + V_m E^m \\
 \frac{\eta_2}{E_{22}} &= \frac{V_{CN}}{E_{22}^{CN}} + \frac{V_m}{E^m} \\
 \frac{\eta_3}{G_{12}} &= \frac{V_{CN}}{G_{12}^{CN}} + \frac{V_m}{G^m}
 \end{aligned} \tag{1}$$

In the above equations, η_1, η_2 and η_3 are the so called efficiency parameters and as mentioned earlier are introduced to account for the size dependent material properties of the plate. These constants are chosen to equal the obtained values of elasticity moduli and shear modulus from the present modified rule of mixtures with the results obtained according to the molecular dynamics simulations

(Shen 2011). In Eq. (1), E_{11}^{CN} , E_{22}^{CN} and G_{12}^{CN} are the elasticity moduli and shear modulus of SWCNTs, respectively. Furthermore, E^m and G^m indicate the corresponding properties of the isotropic matrix.

In Eq. (1), volume fraction of CNTs and matrix are denoted by V_{CN} and V_m , respectively, which satisfy the condition

$$V_{CN} + V_m = 1 \tag{2}$$

The effective Poisson ratio depends weakly on position (Shen 2011) and is expressed as

$$\nu_{12} = V_{CN}^* \nu_{12}^{CN} + V_m \nu^m \tag{3}$$

Conventional rule of mixtures approach is used to obtain the equivalent mass density of the composite media which reads (Wang and Shen 2011, 2012a)

$$\rho = V_{CN} \rho^{CN} + V_m \rho^m \tag{4}$$

where in the above equation, ρ^{CN} and ρ^m are the mass density of the constituents.

First order shear deformation theory (FSDT) of plates suitable for moderately thick and thick plates is used in this study to estimate the kinematics of the plate (Reddy 2003). According to the FSDT, displacement components of the plate may be written in terms of characteristics of the mid-surface of the plate and cross section rotations as

$$\begin{aligned} u(x, y, z, t) &= u_0(x, y, t) + z\varphi_x(x, y, t) \\ v(x, y, z, t) &= v_0(x, y, t) + z\varphi_y(x, y, t) \\ w(x, y, z, t) &= w_0(x, y, t) \end{aligned} \tag{5}$$

In the above equation u, v , and w are the through-the-length, through-the-width and through-the-thickness displacements, respectively. Mid-plane characteristics of the plate are designated with a subscript 0. Besides, transverse normal rotations about the x and y axes are denoted by φ_y and φ_x , respectively.

Following the FSDT, in-plane strain components are written in terms of mid-plane strains and change in curvatures. Besides, through-the-thickness shear strain components are assumed to be constant. Therefore, one may write

$$\begin{Bmatrix} \varepsilon_{xx} \\ \varepsilon_{yy} \\ \gamma_{xy} \\ \gamma_{xz} \\ \gamma_{yz} \end{Bmatrix} = \begin{Bmatrix} \varepsilon_{xx0} \\ \varepsilon_{yy0} \\ \gamma_{xy0} \\ \gamma_{xz0} \\ \gamma_{yz0} \end{Bmatrix} + z \begin{Bmatrix} \kappa_{xx} \\ \kappa_{yy} \\ \kappa_{xy} \\ \kappa_{xz} \\ \kappa_{yz} \end{Bmatrix} \tag{6}$$

To account for the large deflection of the plate in free vibration regime, von Kármán type of geometrical nonlinearity is used. Accordingly, the mid-surface components of strain take the form

$$\begin{Bmatrix} \varepsilon_{xx0} \\ \varepsilon_{yy0} \\ \gamma_{xy0} \\ \gamma_{xz0} \\ \gamma_{yz0} \end{Bmatrix} = \begin{Bmatrix} u_{0,x} + 0.5w_{0,x}^2 \\ v_{0,y} + 0.5w_{0,y}^2 \\ u_{0,y} + v_{0,x} + w_{0,x}w_{0,y} \\ \varphi_x + w_{0,x} \\ \varphi_y + w_{0,y} \end{Bmatrix} \tag{7}$$

and the components of change in curvature compatible with the FSDT are

$$\begin{Bmatrix} \kappa_{xx} \\ \kappa_{yy} \\ \kappa_{xy} \\ \kappa_{xz} \\ \kappa_{yz} \end{Bmatrix} = \begin{Bmatrix} \varphi_{x,x} \\ \varphi_{y,y} \\ \varphi_{x,y} + \varphi_{y,x} \\ 0 \\ 0 \end{Bmatrix} \tag{8}$$

where in the above equations $()_{,x}$ and $()_{,y}$ denote the derivatives with respect to the x and y directions, respectively.

For linear elastic materials, stress field may be written as a linear function of strain field as

$$\begin{Bmatrix} \sigma_{xx} \\ \sigma_{yy} \\ \tau_{yz} \\ \tau_{xz} \\ \tau_{xy} \end{Bmatrix} = \begin{bmatrix} Q_{11} & Q_{12} & 0 & 0 & 0 \\ Q_{12} & Q_{22} & 0 & 0 & 0 \\ 0 & 0 & Q_{44} & 0 & 0 \\ 0 & 0 & 0 & Q_{55} & 0 \\ 0 & 0 & 0 & 0 & Q_{66} \end{bmatrix} \begin{Bmatrix} \varepsilon_{xx} \\ \varepsilon_{yy} \\ \gamma_{yz} \\ \gamma_{xz} \\ \gamma_{xy} \end{Bmatrix} \tag{9}$$

Here Q_{ij} 's ($i, j = 1, 2, 4, 5, 6$) are the reduced material stiffness coefficients compatible with the plane-stress conditions and are obtained as follow

$$\begin{aligned} Q_{11} &= \frac{E_{11}}{1 - \nu_{12}\nu_{21}}, \quad Q_{22} = \frac{E_{22}}{1 - \nu_{12}\nu_{21}}, \\ Q_{12} &= \frac{\nu_{21}E_{11}}{1 - \nu_{12}\nu_{21}} \\ Q_{44} &= G_{23}, \quad Q_{55} = G_{13}, \quad Q_{66} = G_{12} \end{aligned} \tag{10}$$

The governing equations for the nonlinear free vibration analysis of a plate may be obtained according to the Hamilton principle (Reddy 2003). For the nonlinear free vibration problem, where the external forces are absent, Hamilton principle takes the form

$$\int_{t_1}^{t_2} \delta(U - T) dt = 0 \tag{11}$$

$$t = t_1, t_2: \delta u_0 = \delta v_0 = \delta w_0 = \delta \varphi_x = \delta \varphi_y = 0$$

where δU is the virtual strain energy of the FG-CNTRC plate which may be calculated as

$$\delta U = \int_{-0.5a}^{+0.5a} \int_{-0.5b}^{+0.5b} \int_{-0.5h}^{+0.5h} (\sigma_{xx}\delta\varepsilon_{xx} + \sigma_{yy}\delta\varepsilon_{yy} + \tau_{xy}\delta\gamma_{xy} + \kappa\tau_{xz}\delta\gamma_{xz} + \kappa\tau_{yz}\delta\gamma_{yz}) dz dy dx \tag{12}$$

Where the shear correction factor is set to $\kappa = 5/6$. Also δT is the variation of kinetic energy of the plate which also may be written as

$$\delta T = \int_{-0.5a}^{+0.5a} \int_{-0.5b}^{+0.5b} \int_{-0.5h}^{+0.5h} \rho(z) (\dot{u}\delta\dot{u} + \dot{v}\delta\dot{v} + \dot{w}\delta\dot{w}) dz dy dx \tag{13}$$

3. Solution procedure

While the complete set of nonlinear equations and the associated boundary conditions for the nonlinear free vibration problem may be achieved through the application of Green-Gauss theorem to the expression (11), energy based methods also may be used to deduce the governing equations associated to the Eq. (11). In the present research,

the conventional Ritz method with Chebyshev basis polynomials is used to extract the motion equations in a matrix representation. Accordingly, each of the essential variables may be expanded via Chebyshev polynomials and auxiliary functions such that

$$\begin{aligned}
 u_0(x, y, t) &= R^u(x, y) \sum_{i=1}^{N_x} \sum_{j=1}^{N_y} U_{ij}(t) P_i(x) P_j(y) \\
 v_0(x, y, t) &= R^v(x, y) \sum_{i=1}^{N_x} \sum_{j=1}^{N_y} V_{ij}(t) P_i(x) P_j(y) \\
 w_0(x, y, t) &= R^w(x, y) \sum_{i=1}^{N_x} \sum_{j=1}^{N_y} W_{ij}(t) P_i(x) P_j(y) \\
 \varphi_x(x, y, t) &= R^x(x, y) \sum_{i=1}^{N_x} \sum_{j=1}^{N_y} X_{ij}(t) P_i(x) P_j(y) \\
 \varphi_y(x, y, t) &= R^y(x, y) \sum_{i=1}^{N_x} \sum_{j=1}^{N_y} Y_{ij}(t) P_i(x) P_j(y)
 \end{aligned} \tag{14}$$

where in the above equation $P_i(x)$ and $P_j(y)$ are the i -th and j -th Chebyshev polynomials of the first kind which are defined by

$$\begin{aligned}
 P_i(x) &= \cos((i - 1)\arccos(2x/a)) \\
 P_j(y) &= \cos((j - 1)\arccos(2y/b))
 \end{aligned} \tag{15}$$

Besides, functions $R^\alpha(x, y), \alpha = u, v, w, x, y$ are the boundary functions corresponding to the essential boundary conditions. It is known that in Ritz family methods, adoption of a shape function depends only on the essential boundary condition. Three types of boundary conditions are used in this study, i.e., clamped (C), simply supported type one (S) and simply supported type two (S^*). For a clamped edge, all of the in-plane and out-of-plane essential variables are restrained. For a simply supported edge of type one, all of the three displacement components are restrained at the support. For a simply supported edge of type two, normal, tangential and lateral displacements and tangential slope are restrained at the supports. Therefore, the boundary conditions for a completely clamped plate may be written as

$$\begin{aligned}
 x = \pm a/2: u_0 = v_0 = w_0 = \varphi_x = \varphi_y = 0 \\
 y = \pm b/2: u_0 = v_0 = w_0 = \varphi_x = \varphi_y = 0
 \end{aligned} \tag{16}$$

For a type one simply supported plate

$$\begin{aligned}
 x = \pm a/2: u_0 = v_0 = w_0 = 0 \\
 y = \pm b/2: u_0 = v_0 = w_0 = 0
 \end{aligned} \tag{17}$$

and for a type two simply supported plate

$$\begin{aligned}
 x = \pm a/2: u_0 = v_0 = w_0 = \varphi_y = 0 \\
 y = \pm b/2: u_0 = v_0 = w_0 = \varphi_x = 0
 \end{aligned} \tag{18}$$

The shape functions of the Ritz method should be chosen according to the above essential variables. All of the Chebyshev functions are nonzero at both ends of the interval. Therefore, auxiliary functions $R^\alpha, \alpha = u, v, w, x, y$ should satisfy the essential boundary conditions on each edge of the plate. Each of the functions

$R^\alpha, \alpha = u, v, w, x, y$ may be written as

$$R^\alpha(x, y) = \left(1 + \frac{2x}{a}\right)^p \left(1 - \frac{2x}{a}\right)^q \left(1 + \frac{2y}{b}\right)^r \left(1 - \frac{2y}{b}\right)^s \tag{19}$$

Each of the variables p, q, r and s depends on the essential boundary conditions and are equal to zero or one. The present research focuses on plates which are clamped all around or simply supported all around. Therefore the auxiliary functions for each of the three cases are as follows:

For a completely clamped (CCCC) plate

$$\begin{aligned}
 R^u(x, y) &= \left(1 + \frac{2x}{a}\right) \left(1 - \frac{2x}{a}\right) \left(1 + \frac{2y}{b}\right) \left(1 - \frac{2y}{b}\right) \\
 R^v(x, y) &= \left(1 + \frac{2x}{a}\right) \left(1 - \frac{2x}{a}\right) \left(1 + \frac{2y}{b}\right) \left(1 - \frac{2y}{b}\right) \\
 R^w(x, y) &= \left(1 + \frac{2x}{a}\right) \left(1 - \frac{2x}{a}\right) \left(1 + \frac{2y}{b}\right) \left(1 - \frac{2y}{b}\right) \\
 R^x(x, y) &= \left(1 + \frac{2x}{a}\right) \left(1 - \frac{2x}{a}\right) \left(1 + \frac{2y}{b}\right) \left(1 - \frac{2y}{b}\right) \\
 R^y(x, y) &= \left(1 + \frac{2x}{a}\right) \left(1 - \frac{2x}{a}\right) \left(1 + \frac{2y}{b}\right) \left(1 - \frac{2y}{b}\right)
 \end{aligned} \tag{20}$$

For a plate which is simply supported all around (SSSS)

$$\begin{aligned}
 R^u(x, y) &= \left(1 + \frac{2x}{a}\right) \left(1 - \frac{2x}{a}\right) \left(1 + \frac{2y}{b}\right) \left(1 - \frac{2y}{b}\right) \\
 R^v(x, y) &= \left(1 + \frac{2x}{a}\right) \left(1 - \frac{2x}{a}\right) \left(1 + \frac{2y}{b}\right) \left(1 - \frac{2y}{b}\right) \\
 R^w(x, y) &= \left(1 + \frac{2x}{a}\right) \left(1 - \frac{2x}{a}\right) \left(1 + \frac{2y}{b}\right) \left(1 - \frac{2y}{b}\right) \\
 R^x(x, y) &= 1 \\
 R^y(x, y) &= 1
 \end{aligned} \tag{21}$$

For a plate which is simply supported all around ($S^*S^*S^*S^*$)

$$\begin{aligned}
 R^u(x, y) &= \left(1 + \frac{2x}{a}\right) \left(1 - \frac{2x}{a}\right) \left(1 + \frac{2y}{b}\right) \left(1 - \frac{2y}{b}\right) \\
 R^v(x, y) &= \left(1 + \frac{2x}{a}\right) \left(1 - \frac{2x}{a}\right) \left(1 + \frac{2y}{b}\right) \left(1 - \frac{2y}{b}\right) \\
 R^w(x, y) &= \left(1 + \frac{2x}{a}\right) \left(1 - \frac{2x}{a}\right) \left(1 + \frac{2y}{b}\right) \left(1 - \frac{2y}{b}\right) \\
 R^x(x, y) &= \left(1 + \frac{2y}{b}\right) \left(1 - \frac{2y}{b}\right) \\
 R^y(x, y) &= \left(1 + \frac{2x}{a}\right) \left(1 - \frac{2x}{a}\right)
 \end{aligned} \tag{22}$$

Finally substitution of Eq. (14) into the Eqs. (11) results in an eigenvalue problem as

$$(\mathbf{K}^L + \mathbf{K}^{NL1} + \mathbf{K}^{NL2})\mathbf{X} + \mathbf{M}\ddot{\mathbf{X}} = \mathbf{0} \tag{23}$$

where \mathbf{K}^L is the linear elastic stiffness matrix. The two other stiffness matrices, i.e., \mathbf{K}^{NL1} and \mathbf{K}^{NL2} are nonlinear due to the presence of the von Kármán strains. Matrix \mathbf{K}^{NL1} has elements which are dependent linearly to the unknown displacement vector \mathbf{X} and \mathbf{K}^{NL2} has elements which are dependent quadratically to the unknown displacement vector \mathbf{X} . Besides, \mathbf{M} is mass matrix which is linear. The above system is a non-linear eigenvalue problem which

should be solved using a displacement control strategy. It is also worth-noting that, displacement vector \mathbf{X} contains the time-dependent unknown coefficients $U_{ij}, V_{ij}, W_{ij}, X_{ij}$ and Y_{ij} where $i = 1, 2, \dots, N_x$ and $j = 1, 2, \dots, N_y$.

Considering a periodic vibration with only one harmonic, the vector \mathbf{X} may be expressed as $\mathbf{X} = \hat{\mathbf{X}}\sin(\omega t)$ where ω is the frequency of vibration and the vector $\hat{\mathbf{X}}$ contains value of the nodal displacement parameters at the instant that maximum displacement occurs. Substitution of the approximated displacement vector into the Eq. (23) results in a residue as

$$\mathbf{R} = (\mathbf{K}^L + \hat{\mathbf{K}}^{NL1}\sin(\omega t) + \hat{\mathbf{K}}^{NL2}\sin^2(\omega t))\hat{\mathbf{X}}\sin(\omega t) - \omega^2\mathbf{M}\hat{\mathbf{X}}\sin(\omega t) \quad (24)$$

To eliminate the time parameter t from Eq. (24), the weighted residual method is employed. To this end, Eq. (24) which is a residual vector is multiplied by the weight function $\sin(\omega t)$ term and integrated over the domain $[0, \pi/(2\omega)]$ which results in

$$\left(\mathbf{K}^L + \frac{8}{3\pi}\hat{\mathbf{K}}^{NL1} + \frac{3}{4}\hat{\mathbf{K}}^{NL2}\right)\hat{\mathbf{X}} - \omega^2\mathbf{M}\hat{\mathbf{X}} = \mathbf{0} \quad (25)$$

The above system should be treated as a standard nonlinear eigenvalue problem. The procedure to obtain the nonlinear frequencies is mentioned below:

- 1) At first a linear eigenvalue analysis is carried out to obtain the natural frequencies and the associated mode shapes. After this step, nonlinear free vibration analysis begins.
- 2) An element of the displacement vector $\hat{\mathbf{X}}$ is assumed to be known. In this study when the nodal variable of the \hat{W}_{11} from the linear analysis of step 1 is nonzero, \hat{W}_{11} is considered to be known. Otherwise the known degree of freedom is chosen to be \hat{W}_{12} .
- 3) The eigenvector associated to the linear analysis is scaled up according to the assumed displacement of step (2).
- 4) The nonlinear components of the elastic matrix are computed with the displacement vector of step (3).
- 5) A linear eigenvalue analysis at this step may be done.
- 6) Note that, the obtained results at the end of step (5) are just approximate because of step (3). The procedure of steps (3) to (6) is performed iteratively to reach a converged frequency and the associated eigenvector (mode shape). When convergence is achieved, the nonlinear frequency and the associated mode shape are achieved.

4. Numerical results and discussion

In the present research, nonlinear free vibration of FG-CNTRC rectangular plates with $S^*S^*S^*S^*$, SSSS and CCCC boundary conditions is analysed. Unless otherwise stated, Poly (methyl methacrylate), referred to as PMMA, is selected for the matrix with material properties $E^m = 2.5$ GPa, $\nu^m = 0.34$ and $\rho^m = 1150\text{kg/m}^3$. (10,10) armchair SWCNT is chosen as the reinforcement. Elasticity modulus, shear modulus, Poisson's ratio and mass density of SWCNT are dependent to temperature. However in this study temperature dependency of the constituents is ignored and

Table 2 Mechanical properties of (10,10) armchair SWCNT at reference temperature (Shen and Xiang 2014) (tube length=9.26 nm, tube mean radius=0.68 nm, tube thickness =0.067 nm)

$T[K]$	$E_{11}^{CN}[TPa]$	$E_{22}^{CN}[TPa]$	$G_{12}^{CN}[TPa]$	ν_{12}^{CN}	$\rho^{CN}[kg/m^3]$
300	5.6466	7.0800	1.9445	0.175	1400

material properties are considered at reference temperature $T = 300$ K. Shen and Xiang (2014) reported these properties at reference temperature $T = 300$ K. The magnitudes of $E_{11}, E_{22}, G_{12}, \rho$ and ν_{12} for CNTs at reference temperature are given in Table 2.

Han and Elliot (2007) performed a molecular dynamics simulation to obtain the mechanical properties of nanocomposites reinforced with SWCNT. However in their analysis, the effective thickness of CNT is assumed to be at least 0.34 nm. The thickness of CNT as reported should be at most 0.142 nm (Wang and Zhang 2008). Therefore molecular dynamics simulation of Han and Elliot (2007) is re-examined (Shen 2011). The so-called efficiency parameters, as mentioned earlier, are chosen to match the data obtained by the modified rule of mixtures of the present study and the molecular dynamics simulation results (Shen 2011). For three different volume fractions of CNTs, these parameters are as: $\eta_1 = 0.137$ and $\eta_2 = 1.022$ for $V_{CN}^* = 0.12$. $\eta_1 = 0.142$ and $\eta_2 = 1.626$ for $V_{CN}^* = 0.17$. $\eta_1 = 0.141$ and $\eta_2 = 1.585$ for $V_{CN}^* = 0.28$. For each case, the efficiency parameter η_3 is equal to $0.7\eta_2$. The shear modulus G_{13} is taken equal to G_{12} whereas G_{23} is taken equal to $1.2G_{12}$ (Shen 2011).

In whole of the numerical results, in each direction, 10 shape functions are chosen after the examination of convergence. Furthermore, displacement at the midpoint of the plate is denoted by W .

In this section at first three comparison studies are provided for nonlinear free vibrations of cross-ply laminated plates and also free vibrations of FG-CNTRC plates. Afterwards, parametric studies are given for free vibrations of FG-CNTRC plates.

4.1 Comparison studies

For the first comparison study, nonlinear free vibration of composite laminated plates with cross-ply lamination schemes is compared with the available data in the open literature. It should be mentioned that, in cross-ply lamination schemes, the stiffness components A_{i6}, B_{i6} and $D_{i6}, i = 1, 2$ are absent and therefore the present formulation also may be used for these types of composites. In this analysis, material properties are taken from Singha *et al.* (2009) and are as follows $E_{11}/E_{22} = 40, G_{12}/E_{22} = G_{13}/E_{22} = 0.6, G_{23}/E_{22} = 0.5, \nu_{12} = 0.25$ and $\rho = 1$. A square plate with side to thickness ratio $b/h = 100$ is considered. Lamination scheme is $[0/90/0/90/0]$. Comparison is carried out in Table 3. It is observed that, results of our study are in close agreement with the results of Singha *et al.* (2009) for both CCCC and $S^*S^*S^*S^*$ types of boundary conditions which guarantees the accuracy and correctness of the developed formulation.

Table 3 Comparison of nonlinear to linear frequency ratios, ω_{NL}/ω_L in [0/90/0/90/0] cross-ply square plates with $a/h = 100$. Results of our study are compared with those of Singha *et al.* (2009)

Boundary Conditions	Source	$W/h = 0.2$	$W/h = 0.4$	$W/h = 0.6$	$W/h = 0.8$	$W/h = 1.0$
CCCC	Present	1.0081	1.0321	1.0708	1.1227	1.1861
	Singha <i>et al.</i> (2009)	1.0085	1.0335	1.0739	1.1282	1.1946
S*S*S*S*	Present	1.0321	1.1232	1.2614	1.4339	1.6307
	Singha <i>et al.</i> (2009)	1.0315	1.1210	1.2572	1.4281	1.6237

Table 4 Comparison on the first six frequency parameters with those of Garcia Macias *et al.* (2016) (designated by A) and Zhang *et al.* (2015c) (designated by B). CCCC plates are considered. Frequency parameter is defined as $\hat{\omega}_L = \omega_L a^2 \sqrt{\rho^m h / D^m} / \pi^2$ and plate characteristics are $a/h = 1000$ and $a/b = 1$

Type	$V_{CN}^* = 0.12$			$V_{CN}^* = 0.17$			$V_{CN}^* = 0.28$		
	A	B	Present	A	B	Present	A	B	Present
UD	13.304	13.054	13.2918	16.027	15.792	16.0128	20.017	19.745	19.9988
	14.803	14.382	14.7634	18.087	17.714	18.0338	21.848	21.472	21.7981
	18.686	17.853	17.4764	23.327	22.600	23.0453	26.734	26.017	26.4680
	25.623	23.172	24.8497	32.514	31.432	31.5528	35.729	34.652	34.7780
	35.762	31.900	34.1548	43.722	41.809	43.2888	49.142	45.057	47.0094
	36.386	35.743	36.0224	44.862	43.768	43.6826	54.927	47.702	54.3763
FG-X	16.110	15.875	19.0965	19.429	19.155	19.4121	24.390	24.059	24.3660
	17.455	17.026	17.4158	21.352	20.810	21.2954	26.313	25.703	26.2474
	21.077	20.307	20.8748	26.432	25.419	26.1448	31.547	30.443	31.2386
	27.829	26.627	27.1064	35.680	34.078	34.6887	41.388	39.656	40.3142
	37.991	35.095	36.3646	49.364	45.527	47.1722	56.287	52.073	53.8822
	44.258	36.474	43.8177	53.251	47.365	52.7225	67.053	54.094	66.3747

For the second comparison study, natural frequencies of fully clamped FG-CNTRC plates are obtained and compared with the available data in the open literature. Results of this study are presented in Table 4 and compared with those given by Garcia Macias *et al.* (2016), Zhang *et al.* (2015c). In this study, a very thin square plate, i.e., $a/h = 1000$ is considered. Numerical results are provided for three different volume fraction of CNTs and also two different types of CNT dispersion profiles. It is observed that, results of our study match well with those of Garcia Macias *et al.* (2016), Zhang *et al.* (2015c), especially with those of Garcia Macias *et al.* (2016). This comparison study also approves that, mass and stiffness matrices of FG-CNTRC rectangular plates are evaluated correctly.

As mentioned in previous sections, large amplitude free vibrations of FG-CNTRC plates are reported by Wang and Shen (2011). For the next comparison study, results obtained by the present formulation are compared with those obtained by Wang and Shen (2011) which are extracted via a two step perturbation technique. Comparison is presented in Table 5. Thick S*S*S*S* non-square plates with $b/h = 10$ are considered. Two aspect ratios are considered that are $a/b = 2$ and 1.5. CNTs are distributed uniformly across the plate thickness and volume fraction of CNTs is set equal to $V_{CN}^* = 0.28$.

It is again observed that, large amplitude frequencies are in reasonable agreement with those of Wang and Shen (2011). Small differences among the results may belong to different plate theories and different solution methods.

4.2 Parametric studies

After validating the proposed formulation, parametric studies are performed to explore the influences of various parameters on the large amplitude frequencies of the plate. In whole of this section, the non-dimensional frequency is defined as $\Omega = \omega a^2 / h \sqrt{\rho^m / E^m}$.

For the first parametric study, Fig. 1 provides the large amplitude free vibration of a CCCC plate with $a/b = 1$ and $a/h = 20$. Results cover four different patterns of CNT dispersion profile and also three different CNT volume fraction. In each figure, large amplitude frequency is provided as a function of the midpoint lateral deflection. The case $W/h = 0$ belongs to the fundamental frequency parameter. It is verified that, with increasing the volume fraction of CNTs, fundamental frequency of the plate increases. This is accepted since with increasing the volume fraction of CNT, flexural stiffnesses of the plate enhances which results into higher stiffness of the plate.

Comparison of different patterns of CNTs also reveal that, fundamental frequency is maximum for plates with FG-X pattern and is minimum for FG-O pattern. Similar to small amplitude frequency, the large amplitude frequency is also maximum for FG-X plate and is minimum for FG-O pattern.

Also with increasing the volume fraction of CNT, nonlinear frequency of the plate increases. It can be further viewed that the large amplitude frequency increases with the increase in amplitude, as expected. However, it is

Table 5 Comparison of nonlinear to linear frequency ratios, ω_{NL}/ω_L in UD-CNTRC $S^*S^*S^*S^*$ plates with $V_{CN}^* = 0.28$ and $b/h = 10$. Results of our study are compared with those of Wang and Shen (2011). Linear frequency parameter is defined as $\Omega_L = \omega_L a^2 \sqrt{\rho^m/E^m}/h$

Aspect ratio	Source	Ω_L	$W/h = 0.2$	$W/h = 0.4$	$W/h = 0.6$	$W/h = 0.8$	$W/h = 1.0$
$a/b = 2.0$	Present	28.7848	1.0397	1.1511	1.3175	1.5223	1.7529
	Wang and Shen (2011)	27.7839	1.0390	1.1483	1.3102	1.5080	1.7293
$a/b = 1.5$	Present	22.7808	1.0502	1.1893	1.3940	1.6437	1.9244
	Wang and Shen (2011)	22.8989	1.0492	1.1845	1.3809	1.6162	1.8759

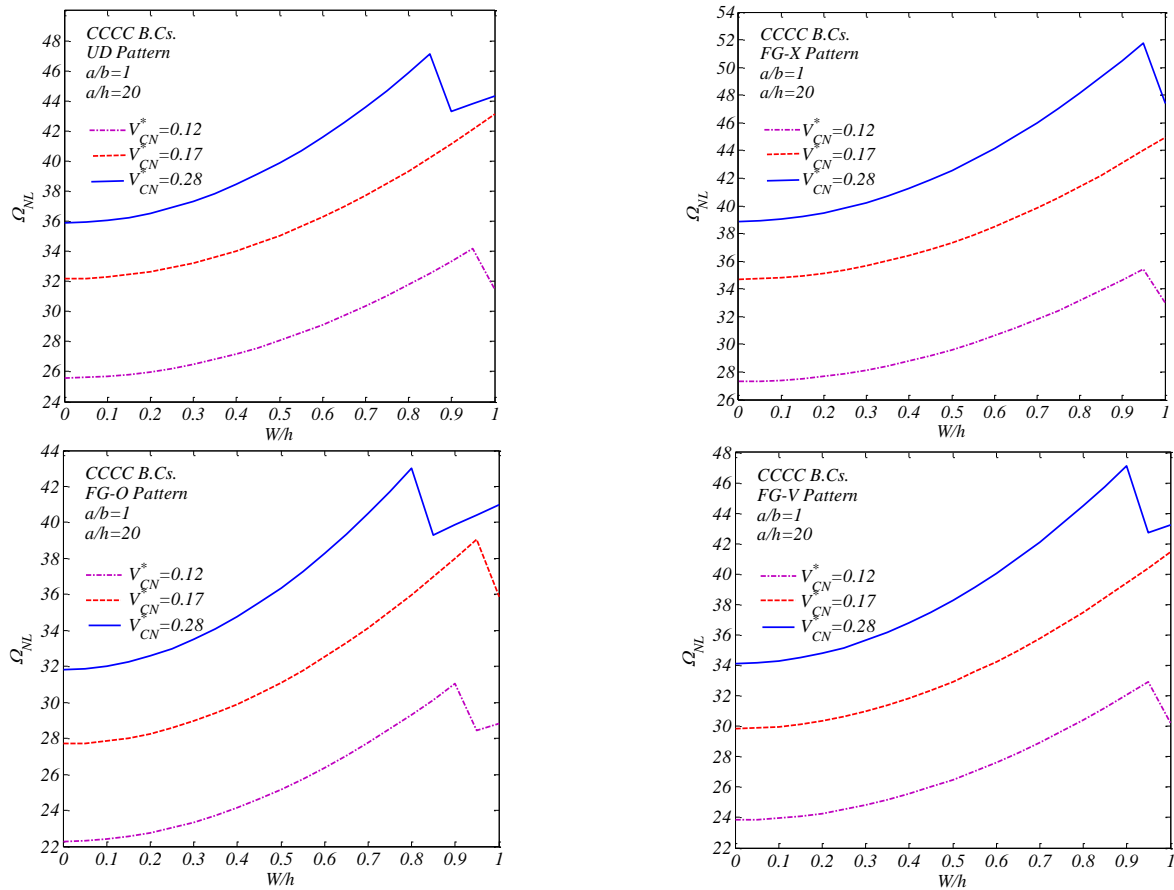


Fig. 1 Nonlinear free vibration parameter in FG-CNTRC plates with different patterns, different CNT volume fraction, $a/b = 1$, $b/h = 20$ and CCCC boundary conditions

noticed that there is a sudden drop in the increasing frequency trend at certain higher amplitude and then gradually increases with further increase in amplitude exhibiting hardening behavior.

This is possibly attributed to the change in stiffness values, and thus leading to the redistribution of mode shapes associated with certain level of amplitudes of vibration, losing symmetry and shifting the maximum displacement towards one side of the plate. Results of Fig. 1 reveal that, among the three different volume fraction of CNTs, the redistribution phenomenon takes place for plates with $V_{CN}^* = 0.28$ in lower amplitudes and for $V_{CN}^* = 0.17$ for higher amplitudes.

Also among the four possible patterns of CNTs, mode redistribution takes place for lower amplitudes in FG-O plates and at higher amplitudes for FG-X plates.

Since among the three functionally graded patterns of CNTs, FG-X pattern results in higher frequencies, only this type of FG-CNTRC is included in to the subsequent numerical results.

Fig. 2 presents the large amplitude free vibration of SSSS FG-CNTRC plates with two graded patterns of CNTs and three different volume fraction of CNTs. In this parametric study also square plates with $a/h = 20$ are considered. Again it is seen that, similar to CCCC plates, linear and nonlinear frequency increases with the enrichment of matrix with more CNT. Furthermore, small and large amplitude frequencies of FG-X plates are higher than those of UD-CNTRC plates. A comparison on Figs. 1 and 2 reveal that, small and large amplitude frequencies of CCCC plates are higher than SSSS plates when all of the geometrical and physical characteristics are the same. This

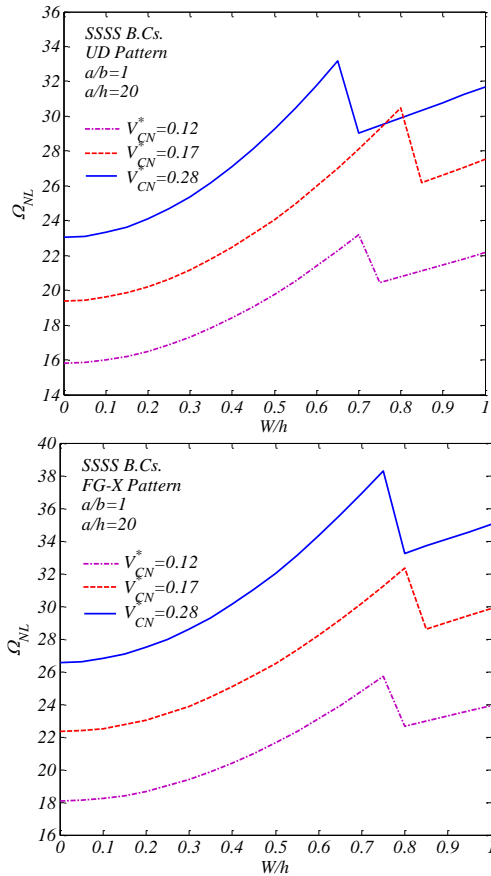


Fig. 2 Nonlinear free vibration parameter in FG-CNTRC plates with different patterns, different CNT volume fraction, $a/b = 1$, $b/h = 20$ and SSSS boundary conditions

is expected since clamping results in higher flexural rigidity in comparison to a simply supported edge. Similar to the observations for CCCC plates in Fig. 1, for SSSS plates also mode redistribution phenomenon takes place which is designated with a sudden drop in frequency amplitude curves. Comparison of Figs. 1 and 2 reveal that, mode redistribution phenomenon takes place in smaller amplitudes for SSSS plates in comparison to CCCC plates.

Fig. 3 aims to analyse the effect of thickness ratio on large amplitude frequencies of the plate. In this example CCCC plates with $V_{CN}^* = 0.17$ and two different CNT dispersion profiles are considered. It is seen that thickness ratio a/h changes the small and large amplitude frequency parameters. This property is observed in shear deformable plate theories. In classical plate theory where the shear strains are ignored, non-dimensional frequency parameter is independent of the thickness ratio.

Fig. 4 analyses the influence of aspect ratio on the linear and nonlinear frequencies of CCCC plates with $a/h = 40$ and different pattern of CNTs.

Four different aspect ratios are considered that are $b/a = 0.5, 0.6, 0.8$ and 1 . Recalling the definition of frequency parameter, it may be concluded that, with increasing the width of the plate, fundamental frequency of the plate decreases and also large amplitude frequency of the plate decreases. For rectangular plates, similar to the

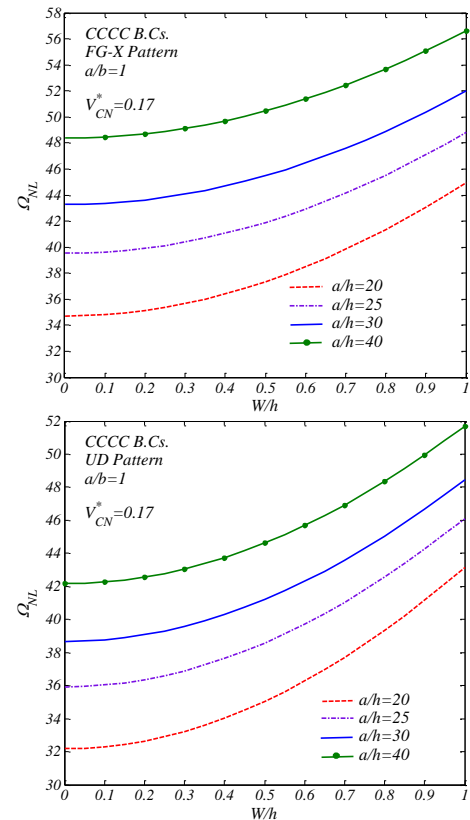


Fig. 3 Nonlinear free vibration parameter in CCCC FG-CNTRC plates with UD and FG-X patterns, $V_{CN}^* = 0.17$, $a/b = 1$ and different side to thickness ratios

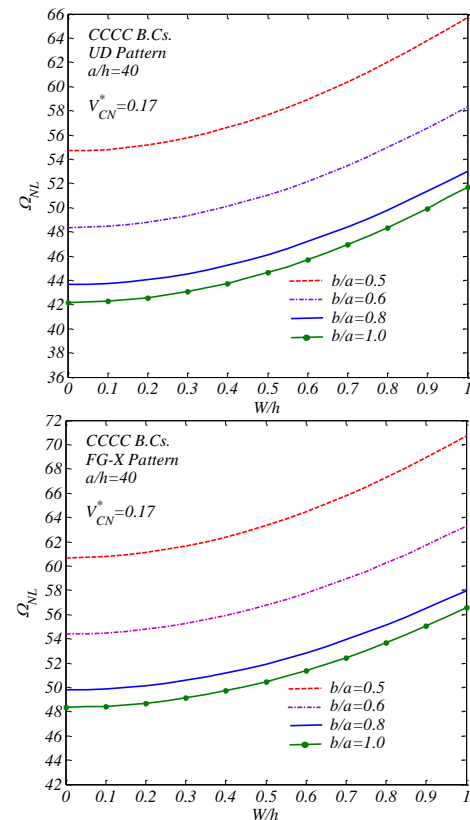


Fig. 4 Nonlinear free vibration parameter in CCCC FG-CNTRC plates with UD and FG-X patterns, $V_{CN}^* = 0.17$, $a/h = 40$ and different aspect ratios

observation of square plates, frequencies of FG-X plates are higher than UD plates.

5. Conclusions

Large amplitude free vibration of FG-CNTRC rectangular plates is investigated in the present research. Formulation is based on a first order shear deformation plate theory which takes into account the von Kármán type of strain-displacement relations to capture the large deformation effect. CNTs are distributed across the plate thickness uniformly or according to a prescribed functionally graded pattern. Properties of the composite media are evaluated by means of a refined rule of mixtures approach which contains efficiency parameters. The governing equations of the system are obtained using the Ritz method whose shape functions are estimated with the aid of Chebyshev polynomials. A nonlinear eigenvalue problem is established and solved by means of a displacement control strategy. Numerical results are first validated for simpler cases and then give new data for FG-CNTRC plates with all edges clamped or simply supported. Results of this study show that, small and large amplitude frequencies of the plate increase with increasing the volume fraction of CNT. Furthermore, among the four different cases of CNT dispersion profiles, FG-X pattern results in higher frequencies and FG-O pattern results in lower frequencies. For both CCCC and SSSS plates, the mode redistribution phenomenon takes place. In such case, the maximum amplitude moves from center to one side of the plate which is also distinguished by a sudden drop in frequency amplitude curves. This phenomenon takes place at lower amplitudes for SSSS plates in comparison to CCCC plates.

References

- Fan, Y. and Wang, H. (2016), "Nonlinear dynamics of matrix-cracked hybrid laminated plates containing carbon nanotube-reinforced composite layers resting on elastic foundations", *Nonlin. Dyn.*, **84**, 1181-1199.
- Fidelus, J.D., Wiesel, E., Gojny, F.H., Schulte, K. and Wagner, H.D. (2005), "Thermo-mechanical properties of randomly oriented carbon/epoxy nanocomposites", *Compos. Part A-Appl. S*, **36**, 1555-1561.
- Garcia-Macias, E., Castro-Triguero, R., Flores, E.I.S., Friswell, M.I. and Gallego, R. (2016), "Static and free vibration analysis of functionally graded carbon nanotube reinforced skew plates", *Compos. Struct.*, **140**, 473-590.
- Han, Y. and Elliot, J. (2007), "Molecular dynamics simulations of the elastic properties of polymer/carbon nanotube composites", *Comput. Mater. Sci.*, **39**, 315-323.
- Kiani, Y. (2016a), "Free vibration of carbon nanotube reinforced plates integrated with piezoelectric layers", *Comput. Math. Appl.*, **72**, 2433-2449.
- Kiani, Y. (2016b), "Free vibration of FG-CNT reinforced composite skew plates", *Aerosp. Sci. Technol.*, **58**, 178-188.
- Kiani, Y. (2016c), "Shear buckling of FG-CNT reinforced composite plates using Chebyshev-Ritz method", *Compos. Part B-Eng*, **105**, 176-187.
- Kiani, Y. (2017a), "Free vibration of carbon nanotube reinforced composite plate on point supports using Lagrangian multipliers", *Meccanica*, **52**, 1353-1367.
- Kiani, Y. (2017b), "Buckling of FG-CNT-reinforced composite plates subjected to Parabolic Loading", *Acta Mech.*, **228**, 1303-1319.
- Kiani, Y. (2017c), "Thermal post-buckling of FG-CNT reinforced composite plates", *Compos. Struct.*, **159**, 299-306.
- Kiani, Y. (2017d), "Free vibration of FG-CNT reinforced composite spherical shell panels using Gram-Schmidt shape functions", *Compos. Struct.*, **159**, 368-381.
- Kwon, H., Bradbury, C.R. and Leparoux, M. (2013), "Fabrication of functionally graded carbon nanotube-reinforced aluminum matrix composite", *Adv. Eng. Mater.*, **13**, 325-329.
- Liew, K.M., Lei, Z.X. and Zhang, L.W. (2015), "Mechanical analysis of functionally graded carbon nanotube reinforced composites: a review", *Compos. Struct.*, **120**, 90-97.
- Malekzadeh, P. and Zarei, A.R. (2014), "Free vibration of quadrilateral laminated plates with carbon nanotube reinforced composite layers", *Thin Wall. Struct.*, **82**, 221-232.
- Mirzaei, M. and Kiani, Y. (2016a), "Free vibration of functionally graded carbon-nanotube-reinforced composite plates with cutout", *Beilstein J. Nanotech.*, **7**, 511-523.
- Mirzaei, M. and Kiani, Y. (2016b), "Free vibration of functionally graded carbon nanotube reinforced composite cylindrical panels", *Compos. Struct.*, **142**, 45-56.
- Mohammadimehr, M. and Alimirzaei, S. (2016), "Nonlinear static and vibration analysis of Euler-Bernoulli composite beam model reinforced by FG-SWCNT with initial geometrical imperfection using FEM", *Struct. Eng. Mech.*, **59**, 431-454.
- Mosallaei Barzoki, A.A., Loghman, A. and Ghorbanpour Arani, A. (2015), "Temperature-dependent nonlocal nonlinear buckling analysis of functionally graded SWCNT-reinforced microplates embedded in an orthotropic elastomeric medium", *Struct. Eng. Mech.*, **53**, 497-517.
- Natarajan, S., Haboussi, M. and Manickam, G. (2014), "Application of higher-order structural theory to bending and free vibration analysis of sandwich plates with CNT reinforced composite facesheets", *Compos. Struct.*, **113**, 197-207.
- Reddy, J.N. (2003), *Mechanics of Laminated Composite Plates and Shells, Theory and Application*, CRC Press, Boca Raton.
- Shen, H.S. (2009), "Nonlinear bending of functionally graded carbon nanotube reinforced composite plates in thermal environments", *Compos. Struct.*, **91**, 9-19.
- Shen, H.S. (2011), "Postbuckling of nanotube-reinforced composite cylindrical shells in thermal environments, part I: axially-loaded shells", *Compos. Struct.*, **93**, 2096-2108.
- Shen, H.S. and Xiang, Y. (2014), "Nonlinear vibration of nanotube-reinforced composite cylindrical panels resting on elastic foundations in thermal environments", *Compos. Struct.*, **111**, 291-300.
- Shi, D.L., Feng, X.Q., Huang, Y.Y., Hwang, K.C. and Gao, H.J. (2004), "The effect of nanotube waviness and agglomeration on the elastic property of carbon nanotube reinforced composites", *J. Eng. Mater. -T, ASME*, **126**, 250-257.
- Singha, M.K. and Daripa, R. (2009), "Nonlinear vibration and dynamic stability analysis of composite plates", *J. Sound Vib.*, **328**, 541-554.
- Tohidi, H., Hosseini-Hashemi, S., Maghsoudpour, A. and Etemadi, S. (2017), "Strain gradient theory for vibration analysis of embedded CNT-reinforced micro Mindlin cylindrical shells considering agglomeration effects", *Struct. Eng. Mech.*, **62**, 551-565.
- Wang, C.Y. and Zhang, L.C. (2008), "A critical assessment of the elastic properties and effective wall thickness of single-walled carbon nanotubes", *Nanotechnol.*, **19**, 075705.
- Wang, Z.X. and Shen, H.S. (2011), "Nonlinear vibration of nanotube-reinforced composite plates in thermal environments",

- Comp. Mater. Sci.*, **50**, 2319-2330.
- Wang, Z.X. and Shen, H.S. (2012), "Nonlinear dynamic response of nanotube-reinforced composite plates resting on elastic foundations in thermal environments", *Nonlin. Dyn.*, **70**, 735-754.
- Wang, Z.X. and Shen, H.S. (2012), "Nonlinear vibration and bending of sandwich plates with nanotube-reinforced composite face sheets", *Compos. Part B - Eng.*, **43**, 411-421.
- Zhang, L.W., Lei, Z.X. and Liew, K.M. (2015), "Computation of vibration solution for functionally graded carbon nanotube-reinforced composite thick plates resting on elastic foundations using the element-free IMLS-Ritz method", *Appl. Math. Comput.*, **256**, 488-504.
- Zhang, L.W., Lei, Z.X. and Liew, K.M. (2015), "Free vibration analysis of functionally graded carbon nanotube-reinforced composite triangular plates using the FSDT and element-free IMLS-Ritz method", *Compos. Struct.*, **120**, 189-199.
- Zhang, L.W., Lei, Z.X. and Liew, K.M. (2015), "Vibration characteristic of moderately thick functionally graded carbon nanotube reinforced composite skew plates", *Compos. Struct.*, **122**, 172-183.

PL